Bull Earthquake Eng (2010) 8:363–385
DOI 10.1007/s10518-009-9155-0

ORIGINAL RESEARCH PAPER

Seismic evaluation of an existing complex RC building

Maja Kreslin · Peter Fajfar

Received: 27 May 2009 / Accepted: 27 August 2009 / Published online: 11 September 2009

Abstract The seismic evaluation of existing buildings is a more difficult task than the seismic design of new buildings. Non-linear methods are needed if realistic results are to be obtained. However, the application to real complex structures of various evaluation procedures, which have usually been tested on highly idealized structural models, is by no means straightforward. In the paper, a practice-oriented procedure for the seismic evaluation of building structures, based on the N2 method, is presented, together with the application of this method to an existing multi-storey reinforced concrete building. This building, which is asymmetric in plan and irregular in elevation, consists of structural walls and frames. It was designed in 1962 for gravity loads and a minimum horizontal loading (2% of the total weight). The main results presented in terms of the global and local seismic demands are compared with the results of non-linear dynamic response-history analyses. As expected, the structure would fail if subjected to the design seismic action according to Eurocode 8. The shear capacity of the structural walls is the most critical. If the shear capacity of these elements was adequate, the structure would be able to survive the design ground motion according to Eurocode 8, in spite of the very low level of design horizontal forces. The applied approach proved to be a feasible tool for the seismic evaluation of complex structures. However, due to the large randomness and uncertainty which are involved in the determination of both the seismic demand and the seismic capacity, only rough estimates of the seismic behaviour of such structures can be obtained.

Keywords Reinforced concrete building · Seismic evaluation · Eurocode8 · N2 method · Pushover analysis · Non-linear dynamic analysis · Seismic capacity

M. Kreslin (✉) · P. Fajfar
Faculty of Civil and Geodetic Engineering, University of Ljubljana, Jamova 2, 1000 Ljubljana, Slovenia
e-mail: maja.kreslin@ikpir.fgg.uni-lj.si

P. Fajfar
e-mail: peter.fajfar@ikpir.fgg.uni-lj.si

1 Introduction

In order to obtain realistic seismic evaluations of existing structures, non-linear methods are needed. The methods, which are based on non-linear response-history, are theoretically correct and represent a long-term trend. However, for the time being, they are still too demanding for everyday practice. Over the last decade, simplified methods for non-linear seismic analysis, which combine the non-linear static (pushover) analysis of a multi degree-of-freedom (MDOF) model, and the response spectrum analysis of an equivalent single-degree-of-freedom (SDOF) model, have become popular. These methods, which have been implemented in recent standards and codes, are intended to achieve a satisfactory balance between required reliability and applicability for everyday design use. The availability of practical non-linear analysis methods for the determination of seismic demand and of empirical data about the seismic capacity of structural elements means that evaluations of the seismic behaviour of structures subjected to strong ground motion can be much more rational and reliable than those corresponding to old practices, which are mainly based on linear analysis methods. However, even with the more advanced methods which are readily available today, only rough estimates of the seismic behaviour can be obtained due to large randomness and uncertainty related to both seismic demand and capacity. An overview of the concepts, philosophy and approaches for the seismic evaluation of existing reinforced concrete RC) structures is presented in Ghobarah (2000).

In the literature, mostly relatively simple structures are used as test examples for demonstrating the application of different approaches to seismic analysis and evaluation (e.g. Lupoi et al. 2004; Panagiotakos and Fardis 2004; Bardakis and Dritsos 2007). If the evaluation approaches are applied to a complex structure, a lot of problems occur at different stages of the evaluation process, which need professional assessment and reasonable solutions. The aim of the paper is to demonstrate the application of an advanced practice-oriented approach for seismic evaluation to a complex reinforced concrete (RC) building structure. The approach is based on the N2 method (Fajfar 2000). The assessment procedure does not strictly follow any code, although several steps are in compliance with Eurocode 8 (CEN 2004, 2005). The main deviation from any code procedure occurs in the use of best estimates for different parameters (e.g. the material characteristics and capacities of structural members) rather than low fractile values. The intention of the applied procedure was to obtain realistic information about the seismic resistance of the investigated building.

In the paper, first a brief summary of the approach used for seismic evaluation is summarized. The approach is then applied to an existing irregular multi-storey RC building. The main results, presented in terms of the global and local seismic demands, are compared with the results of non-linear dynamic response-history analyses. Capacities at the element level are determined according to Eurocode 8-3 (CEN 2005). For comparison, the shear capacities were also determined by using some other procedures and data available in the literature. Finally, the seismic structural behaviour was estimated by comparing the demand and capacity at the local and global structural level.

2 Summary of the evaluation procedure

The seismic assessment of a structural system is performed by comparing seismic demand and capacity for different limit states. (Note that in European terminology the term “limit state” has a similar meaning as the term “performance level”, which is used in US terminology).

Seismic demand is determined by the analysis of a structural model subjected to a specified ground motion. Since the expected structural behaviour during strong ground motion is inelastic, it is preferable to perform a non-linear analysis. The relevant results of such an analysis are the deformations of the structure and of its elements. The seismic capacity of the whole structure depends on the capacities of its individual elements. For ductile elements, the capacity should be expressed in terms of deformation, whereas strength is important for brittle elements.

2.1 Determination of seismic demand

The extended N2 method was used for the determination of demand. The basic version of the N2 method has been implemented in Eurocode 8 (hereinafter referred to as "EC8"). The method is based on pushover analysis. Seismic demand is determined from inelastic spectra and depends on the period of the idealized equivalent SDOF system. The details of the procedure are described elsewhere (Fajfar 2000) and will therefore not be repeated here.

In the N2 method, as well as in other similar methods, the transformation from a MDOF to an equivalent SDOF system is based on the assumption of a time-invariant displacement shape. This assumption represents the major limitation of the applicability of the method. It works well in the case of planar structural models where the higher modes have relatively little influence. In the case of asymmetric building structures, represented by 3D structural models, several modes may substantially contribute to the response, and the torsional effects may not be properly taken into account by a straightforward extension of the N2 method to 3D models. The results of recent parametric studies (Fajfar et al. 2005) suggest that in the majority of cases an upper limit for torsional effects can be estimated by a linear dynamic (spectral) analysis. Furthermore, it has been observed that any favourable torsional effect on the stiff side, i.e. any reduction of displacements compared to the counterpart symmetric building, which may arise from elastic analysis, will probably decrease or may even disappear in the inelastic range. Based on these observations, it was proposed that the results obtained by pushover analysis of a 3D structural model be combined with the results of a linear dynamic (spectral) analysis (Fajfar et al. 2005). Note that the same or a similar approach for the estimation of torsional effects can also be applied to other pushover-based methods.

2.2 Determination of seismic capacity

Seismic capacity can be clearly defined at the element level. Usually, empirical or semi-empirical values are provided for the capacities in terms of deformation and strength. In Eurocode 8-3 (hereinafter referred to as EC8-3, CEN 2005), in the case of RC elements empirical formulas are provided for ultimate chord rotation, which corresponds to the Near Collapse (NC) limit state, and for shear strength. The EC8-3 formulas were used in this study, as explained in more detail in Sect. 7.

The flexural capacity (ultimate rotations) can also be determined according to other approaches available in the literature. Peruš et al. (2006) proposed a non-parametric approach for the determination of the flexural capacity of RC columns. Since the critical structural elements in the investigated building are structural walls, which are not included in the two databases, it was not possible to use the approach proposed by Peruš et al. in this study. Data on the capacity of structural elements are also provided in FEMA 356 (2000). Values for the acceptable plastic hinge rotations of RC elements are presented as a function of the type of

Fig. 1 Failure of a structural wall during the 2009 L'Aquila earthquake. Photographs by M. Rozman and K. Rejec, 2009

element, the performance level, the component type, the confined boundary, and the axial and shear force levels.

In addition to the EC8-3 model, several other models are available for the determination of the shear strength of RC members. In this paper, four models proposed in literature were used for comparison: ACI 318-08 (2007), Sezen and Moehle (2005), Priestley et al. (1994), and Kowalsky and Priestley (2000). In ACI 318 a special formula is provided for structural walls which are the critical structural elements in the case of the building investigated in this study. The other three models were basically derived for columns. However, the latter two models have also been used for RC hollow bridge piers (Calvi et al. 2005; Isaković et al. 2008), which are similar to cores (walls). Some of these shear models depend on displacement ductility, and they are quite sensitive to small variation in the input data. For this reason it is difficult to apply these shear models to estimate the displacement at which shear failure occurs (Sezen and Moehle 2005).

At the system level, there is a lack of a generally accepted definition of seismic capacity at different limit states. In this study, it was assumed that the NC limit state of the whole structure coincides with the NC limit state of the first important element of the structural system, i.e. a column or a structural wall. Such a definition is practical but conservative. Firstly, the NC limit state at the element level does not represent the collapse of the element (in the case of flexural behaviour it is usually defined at a 20% drop in strength). Secondly, the failure of a single column or a wall usually does not signify collapse of the system. For illustration, a RC building in the L'Aquila area is shown in Fig. 1. During the 2009 L'Aquila earthquake this building with structural walls was heavily damaged. The majority of the lightly reinforced walls failed. However, the structure was still far from collapsing.

3 Description of the building

The building is an existing multi-storey RC structure, which is located in Ljubljana, Slovenia (Fig. 2). It was designed in 1962 for gravity loads and for a minimum horizontal loading which amounted to 2% of gravity loading. The structural system consists of structural walls (cores) and frames. According to EC8, it is categorized as being non-regular in both elevation and plan. The building is shown in cross-section in Fig. 3, and in plan in Fig. 4.

Fig. 2 The investigated multi-storey RC building

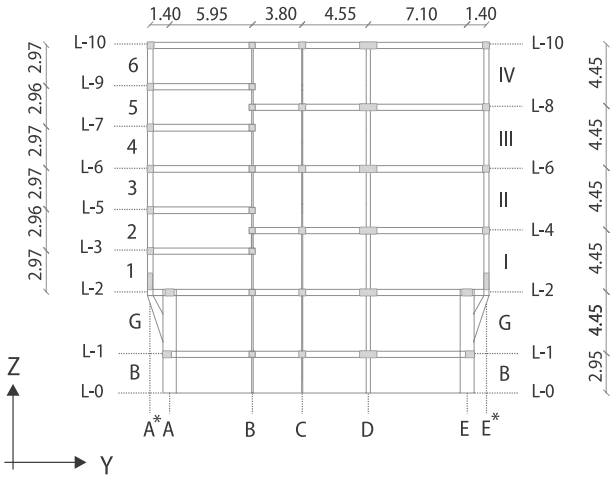

Fig. 3 Typical cross-section of the investigated building, through axis IV. The stories (B, G, 1, 2, 3, 4, 5, 6, I, II, III, IV) and levels (L-0, L-1, …, L-10) are denoted separately

In the analyses, the concrete compression strength and the reinforcement yield stress were assumed to amount to 20–33 MPa for different structure elements (based on material tests performed on elements of the structure), and to 282 MPa (based on the design documentation), respectively. The dimensions and reinforcement of typical structural members (beams, columns, walls) were obtained from the design documentation and from field measurements.

The floor masses and moments of inertia were determined according to EC8. The total mass of the building amounts to 16,400 tons. The structure is symmetric in the *Y* direction. In the *X* direction, the eccentricity between the mass centre and the approximate stiffness centre amounts to about 10%.

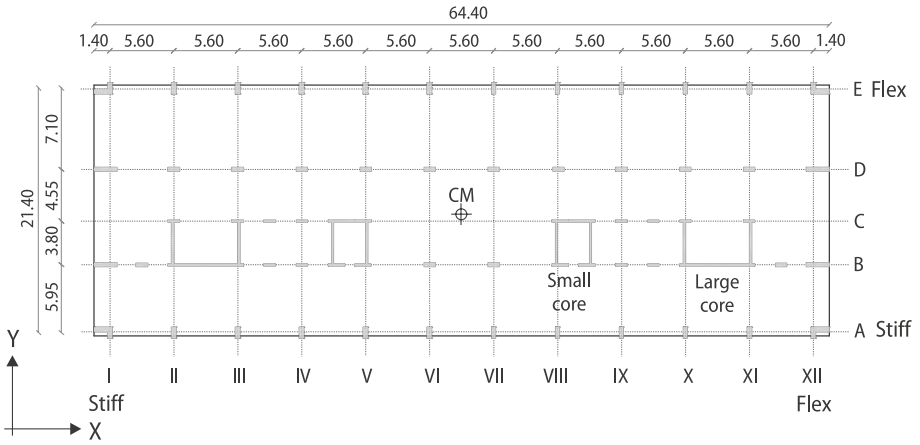

Fig. 4 Plan view of the lower stories. The centres of the storey masses, and the stiff and the flexible sides are marked

4 Mathematical modeling

A relatively simple pseudo-tridimensional mathematical model was chosen for the analyses. The model consists of planar frames and walls, which are connected together by means of rigid diaphragms at the floor levels. In this modelling approach, each column and wall is modelled independently in each of the two directions, and is subjected to independent uni-axial bending, rather than to biaxial bending. Compatibility of the axial deformations in columns belonging to the two frames was not considered. The torsional stiffness of all the elements was neglected. Using this modelling approach, the structural model consists of 4 planar frames in the *X* direction, and 12 such frames in the *Y* direction (see Fig. 4), and of 8 planar walls (each core is represented by a wall in the *X* and *Y* direction). All the structural members (including the walls) were modelled as planar elastic beam elements. Hinge connections were assumed between the frames and the walls.

Masses were concentrated at four levels (B, G, 3-II and 6-IV) which represent the so-called "complete stories", i.e. the stories with continuous floors in the whole area of the plan (Fig. 3). The four masses amount to 2,150, 4,460, 5,740 and 4,080 tons. Alternatively, a model with masses concentrated at all ten levels was also investigated. Since the differences of the results obtained by this model were very similar to the results of the model with four masses, the later one was used in order to avoid problems related to "uncomplete stories".

According to EC8, the elastic flexural and shear stiffness properties of cracked concrete elements may be taken to be equal to one-half of the corresponding stiffness of the uncracked elements, unless a more accurate analysis of the cracked elements is performed. This option was used for the beams and columns, whereas the initial effective stiffnesses of the walls were computed more accurately, based on the results of moment-curvature analyses of their cross-sections. The reduction factors for secant stiffness to the yield point, amounting to between 0.15 and 0.40, were determined. Neither rigid offsets for the interconnecting beams, columns and wall elements, nor the P-delta effect were taken into account in the model. Accidental eccentricity, too, was not taken into account in the analyses presented in this paper. It should be noted, however, that large torsional influences occur if the accidental

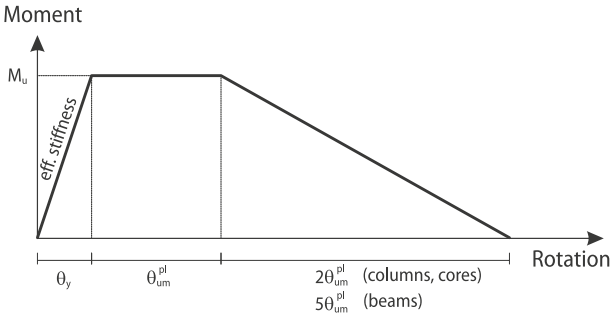

Fig. 5 The moment—rotation envelope for the plastic hinges. Only the plastic part of the rotation applies to the plastic hinge element in PERFORM-3D

eccentricity, required by EC8 (5% of the dimension in plan), is taken into account (Kreslin et al. 2008).

The mathematical model used for the elastic analysis was extended to the non-linear range by introducing one-component plastic rotational hinges at both ends of every planar element (beams, columns and walls). The plastic hinge for flexural behaviour is defined by the moment—rotation relationship. Figure 5 presents the envelope of such plastic hinges, with an effective ('cracked') initial stiffness, and strength degradation after the ultimate rotation is reached. In the case of the PERFORM-3D program (CSI 2006), which was used for the analyses, only plastic rotations apply to the plastic hinge element. The initial elastic part is included in the elastic beam element. It depends on the effective stiffness of the elements. The ultimate plastic rotation was determined according to EC8-3 (Eq. A.3). For the walls, the value of the ultimate plastic rotation for the walls has to be multiplied by a factor of 0.6, taking into account the requirements of EC8-3. Intentionally, no reduction in ultimate deformation capacity due to non-seismic details (see Sect. 7) was taken into account. The aim was to obtain pushover curves with an extended non-linear range which allow testing of different options for capacity without repeating the complete analysis procedure. Of course, the results of analyses are valid only up to the point when the first important structural element fails. The plastic rotation at total collapse was arbitrarily assumed to be equal to twice and five times the plastic ultimate rotation for the columns and walls, and beams, respectively. Since, according to the analyses, the deformation demand was limited, the degrading part of the envelope was of little practical importance. The maximum moment M_u was determined for each element using the moment-curvature analysis, where the axial forces resulting from the vertical loading were considered. The moment—rotation envelope was symmetric (i.e. equal for both senses of the loading) for the plastic hinges in the rectangular columns, and asymmetric for the plastic hinges in all the other elements.

In the study, the PERFORM-3D program (CSI 2006) was used for the pushover analyses and the response-history analyses. This program has been chosen because it is user-friendly and very efficient regarding computation time. Unfortunately, an appropriate hysteretic model for RC elements is not available in this program. Among the available hysteretic models, the bilinear model with stiffness degradation was chosen for modelling the cyclic behaviour (Fig. 6) in the response-history analyses. The unloading and reloading stiffness degradation factor (named "energy degradation factor" in PERFORM) was assumed to be 0.5. This energy factor represents the ratio between the area of the degraded hysteresis loop and the area of the non-degraded loop. The damping matrix was proportional to the mass and the initial

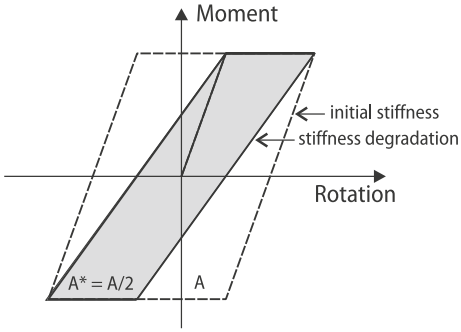

Fig. 6 The bilinear hysteretic model with stiffness degradation, provided in PERFORM. The "energy degradation factor" is assumed to be 0.5

stiffness matrices. 5% damping was assumed in the first and third mode. For the N2 method and modal analyses, 5% damping was taken into account in the elastic spectrum.

In the model, only non-linear behaviour in flexure was considered. It was assumed that the shear capacity of the structural elements was adequate and that shear failures of the structural elements do not occur. As was expected, and was later demonstrated, this assumption was not correct. Nevertheless, it was used to obtain pushover curves with an extended non-linear range, which allow the checking of different scenarios. The shear capacities of the most critical elements were introduced in the assessment stage, where the shear strength of the critical elements was compared with shear demand. Another, more sophisticated possibility would be to use a mathematical model with interacting element models representing inelastic flexural and shear response. Such models, which are much more complex than the simple model used in this study, have been developed (see, e.g., Mergos and Kappos 2008, they provide also a list of previous models).

5 Ground motions

The building is located in Ljubljana, and the local soil has been characterized as type C. Its importance factor amounts to 1.2 (it is used as a school building). Considering the seismic hazard map, the design ground acceleration amounts to $1.2 \times 0.25\,\mathrm{g} = 0.3\,\mathrm{g}$. Taking into account the soil factor 1.15, the effective design ground acceleration amounts to $a_g = 0.345$ g. In a normal assessment case, the EC8 spectrum would determine the ground motion. In the investigated case, however, the aim was to compare the results obtained by the simplified pushover based method with the results of response-history analyses. For this reason a set of ten two-component ground motions was selected from the European strong-motion database (Ambraseys et al. 2002). The records were obtained on soil with an average shear wave velocity of 180–360 m/s to a depth of 30 m. The basic data of the records are presented in Table 1. The ground motions were scaled to the spectral acceleration $S_a = 0.33\,\mathrm{g}$ at the average value of the periods of the second and the third mode of the building, $T = 1.55\,s$. The value $S_a(T = 1.55\,\mathrm{s}) = 0.33\,\mathrm{g}$ corresponds to the value in the EC8 elastic acceleration spectrum for ground type C for an effective design ground acceleration $a_g = 0.345\,g$.

The scaled elastic acceleration spectra for individual accelerograms, as well as the mean spectrum and the EC8 spectrum, are shown in Fig. 7. The mean spectrum is well above the EC8 spectrum for periods smaller than the three fundamental periods of the building.

High scaling factors are needed in order to obtain the target spectral acceleration (Table 1). This was one of the reasons to perform a comparative analysis with another set of records

Table 1 List of ground motion records for ground type C (soft soil)

Earthquake	County	Year	Accelerogram	Magnitude (Mb)	Comp.	PGA (g)	Scaling factor
Ionian	Greece	1973	Lefkada-OTE Building	5.6	N–S	0.52	6.67
					E–W	0.25	7.46
Aftershock (Friuli)	Italy	1976	Buia	5.7	N–S	0.11	2.79
					E–W	0.10	4.71
Basso Tirreno	Italy	1978	Patti-Cabina Prima	5.5	N–S	0.07	8.05
					E–W	0.16	6.26
Thessalonika	Greece	1978	Thessaloniki-City Hotel	6.1	N–S	0.14	7.85
					E–W	0.15	9.56
Tabas	Iran	1978	Boshroyeh	6.4	N–S	0.10	2.35
					E–W	0.09	1.87
Alkion	Greece	1981	Korinthos-OTE Building	6.1	N–S	0.23	3.81
					E–W	0.31	8.83
Alkion	Greece	1981	Korinthos-OTE Building	5.7	N–S	0.12	2.81
					E–W	0.12	2.28
Spitak	Armenia	1988	Gukasian	6.5	N–S	0.18	6.79
					E–W	0.18	4.83
Manjil	Iran	1990	Tonekabun	6.2	N–S	0.14	2.05
					E–W	0.09	2.49
Umbro-Marchigiano	Italy	1997	Castelnuovo-Assisi	5.7	N–S	0.16	6.18
					E–W	0.11	4.43

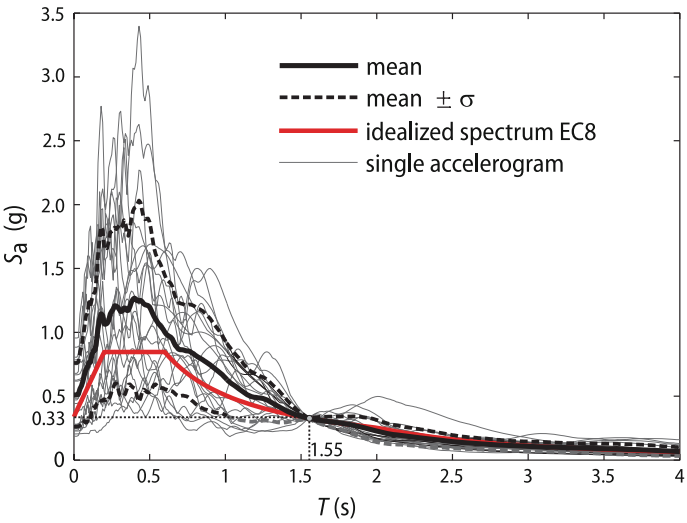

Fig. 7 Elastic spectra for 5% damping, scaled to 0.33 g at the average period of the second and third mode of the building ($T = 1.55$ s). For comparison, the idealized EC8 spectrum for ground type C is presented

representing soil type A. The scaling factors were much lower, whereas the results (not shown here) were qualitatively similar.

Two components of each scaled record were applied simultaneously in the non-linear response-history analyses. For each record two different combinations of the directions of the components were applied, i.e. in the first analysis the first component was applied in the X direction, and the second in the Y direction, whereas in the second analysis the first component was applied in the Y direction and the second in the X direction. So, altogether 20 response-history analyses were performed. In the N2 method, the mean spectrum of the 20 accelerograms (Fig. 7) was used in both horizontal directions.

6 Results of the analyses

The results of the analyses are summarized in this section. The N2 results are compared with the results of non-linear dynamic analyses.

6.1 Periods and modal shapes

The basic modal properties of the building are summarized in Table 2. The three fundamental periods of vibration of the building (considering the cracked element sections described in Sect. 4) amount to 2.03, 1.82 and 1.28 s. The effective masses indicate that the first mode is predominantly torsional, the second mode is translational in the Y direction, and the third mode is predominantly translational in the X direction. Since the first mode is predominantly torsional, the structure is classified as torsionally flexible. Two components of two fundamental mode shapes are shown in Fig. 8. The shapes, which are typical for cantilever beams, indicate that the global behaviour of the structure, at least in the elastic range, is controlled by the cores (walls).

For comparison, the periods for the mathematical model in which the initial stiffnesses of walls were also determined by means of one-half of the corresponding elastic flexural and shear stiffness of the uncracked elements are also presented in Table 2. In this case, about

Table 2 The elastic periods (T) for the basic model with cracked element sections described in Sect. 4 (A), for the model with cracked element sections corresponding to one-half of the corresponding elastic flexural and shear stiffness of the uncracked elements (B), and according to the ambient vibrations test (C)

Mode	(A)				(B)	(C)
	T (s)	$M_{\text{eff,UX}}$ (%)	$M_{\text{eff,UY}}$ (%)	$M_{\text{eff,RZ}}$ (%)	T (s)	T (s)
1	2.03	1	0	62	1.81	0.56
2	1.82	0	62	0	1.59	0.56
3	1.28	65	0	1	1.13	0.40
4	0.51	0	0	18	0.40	
5	0.43	0	19	0	0.33	
6	0.36	16	0	0	0.28	
7	0.24	1	0	12	0.19	
8	0.20	0	13	0	0.16	
9	0.19	11	0	1	0.15	

For the basic model, the effective masses and the effective mass moment (M_{eff}) are also shown

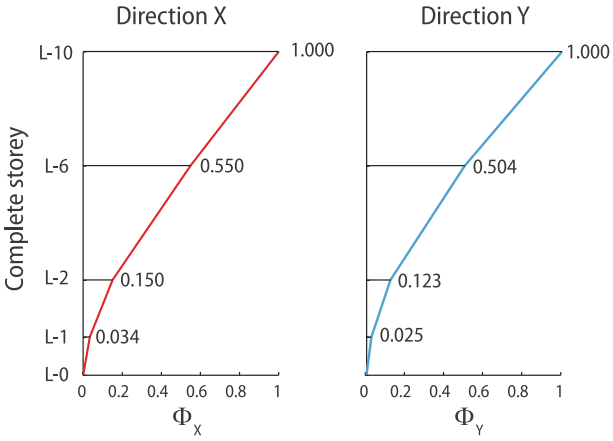

Fig. 8 The fundamental mode shapes in the X direction (the x-components of the third mode shape) and the Y direction (the y-components of the second mode shape)

11–23% smaller periods apply. The effective masses (not included in Table 2) are similar to those of the basic mathematical model.

Mathematical models with cracked cross-sections and without non-structural elements (used in the study presented in this paper) are appropriate for the simulation of vibrations in the case of strong ground motion, whereas in the case of very weak vibrations a much larger effective stiffness applies. For the investigated building, measurements of ambient vibration were performed. The observed periods amounted to 0.56, 0.56 and 0.40 s for the predominantly torsional mode, the predominantly translational mode in the Y direction, and the predominantly translational mode in the X direction, respectively. The results of the ambient vibration measurements indicated that, in the case of very small vibrations, the stiffness of the building is more than ten times greater than that used in the analysis according to the seismic codes. Numerically, it was possible to closely match the results obtained by the ambient vibration test if a model with uncracked cross-sections of the structural elements was used, and if the non-structural elements (mainly infill and partition walls, and façade panels) were included in the mathematical model by means of equivalent diagonals. More details can be found in Kreslin et al. (2006).

6.2 Determination of the target displacement for nonlinear static (pushover) analysis

The target displacements for the two horizontal directions were determined according to the basic N2 method. Pushover analyses of the 3D structural model were performed independently for the X and Y directions. "Fundamental-mode" height-wise distributions of the lateral loads were used, based on the fundamental mode shapes in the corresponding direction, i.e. the x-components of the third mode shape were used in the X direction, and the y-components of the second mode shape were used in the Y direction. The fundamental mode shapes for the X and Y directions and the "modal" force distributions are shown in Figs. 8 and 9. The lateral loads, determined as the product of the mode shape component in a story and the storey mass, were applied at CM (the centre of mass) at each "complete storey" with the + and − sign. The coordinate system is shown in Fig. 4.

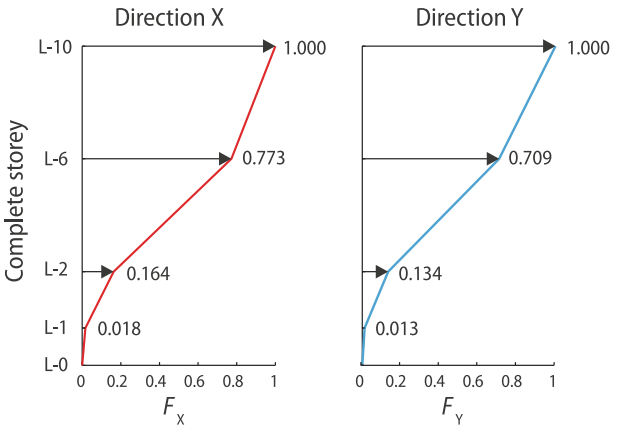

Fig. 9 The fundamental-mode height-wise distributions of lateral loads in the X and Y directions

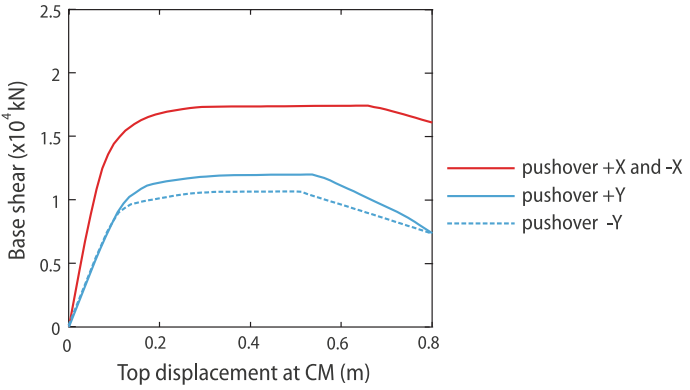

Fig. 10 Pushover curves for both directions

The results of the pushover analyses are shown in Fig. 10 for the positive and negative X and Y directions. The structure is symmetric in the Y direction, so the results for the X direction are the same for the + and − sign. In the Y direction, a lower strength applies to the case of loading in the minus sense. Although the building was designed only for a minimum horizontal loading amounting to 2% of the gravity loading, the maximum strength versus weight ratio amounts to about 10.7 and 6.5% (7.4%) for the X and Y directions, respectively. The value in brackets corresponds to the positive Y direction. (Note that the total mass of the building amounts to 16,400 tons).

For the Y direction, the envelope of the results obtained for the + and − sign will be used at the final stage. In the description of the computational procedure mainly the results for the negative sign of loading will be presented.

The transformation factor Γ for the transformation of the MDOF system to the SDOF system and vice versa amounts to $\Gamma = 1.35$ for both directions. The effective masses amount to $m^* = 7,978$ tons and 7,574 tons for the X and Y directions, respectively. (For formulas, see Fajfar 2000 or EC8.) In Fig. 11, the same curve describes the relation between the base shear and top displacement for the MDOF system (the $d_n - F_b$ relationship) and the equiv-

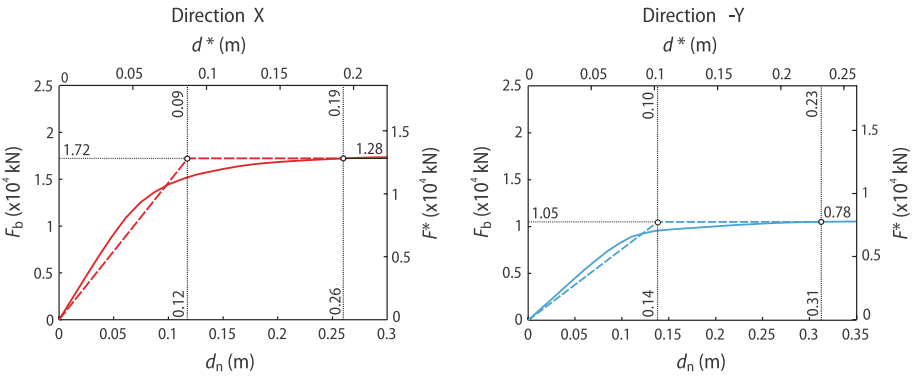

Fig. 11 Pushover curves and bilinear idealizations in the X direction and in the negative Y direction for the MDOF and SDOF systems. The factor between the scales for the MDOF and SDOF system is equal to Γ. The yield strengths, yield displacements and target displacements of the SDOF and MDOF systems are marked

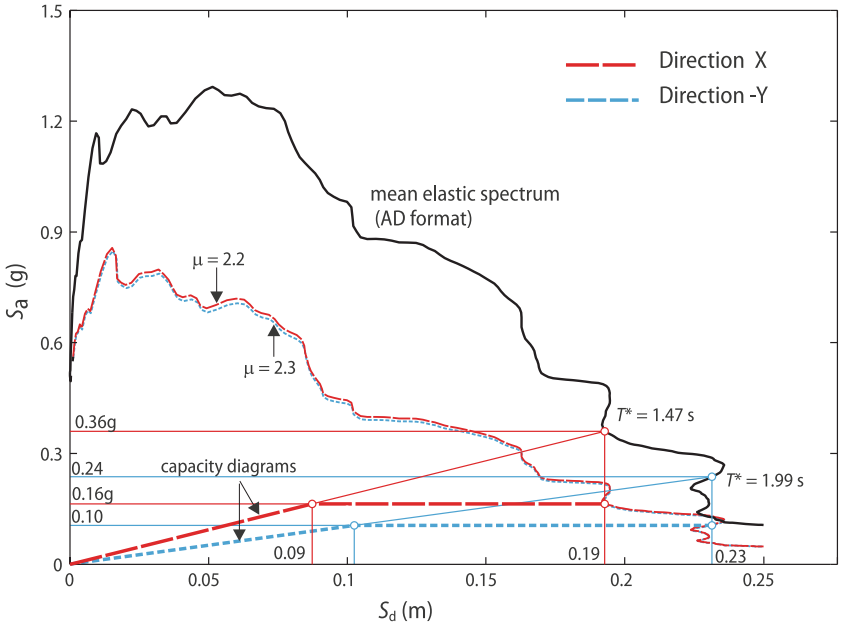

Fig. 12 Elastic and inelastic demand spectra and capacity diagrams in the X direction and in the negative Y direction

alent SDOF system (the d^*–F^* relationship). The factor between the two scales is equal to $\Gamma = 1.35$.

Bilinear idealizations (zero post-yield stiffness) of pushover curves are shown in Fig. 11. The procedure according to EC8, with the iterative determination of the target displacement, was used. The effective periods amount to $T^* = 1.47$ and 1.99 s in the X and negative Y directions, respectively.

The capacity diagrams (Fig. 12) are obtained by dividing the forces of the idealized SDOF system by the equivalent mass. The accelerations at the yield point amount to $F_y^*/m^* = 0.16$ g and 0.10 g for the X and the negative Y directions, respectively. The ground motion was

Table 3 Summary of the SDOF results obtained by the N2 method

Dir.	$F_y/(m \cdot g)$	m^* (t)	Γ	F_y^* (kN)	d_y^*(cm)	T^* (s)	S_{ay} (g)	S_{ae} (g)	$q_u = \mu$	d_{et}^* (cm)	d_t^* (cm)
X	0.107	7,980	1.35	12,800	8.7	1.47	0.16	0.36	2.21	19.3	19.3
$+Y$	0.073	7,570	1.35	8,800	11.4	1.97	0.12	0.24	2.04	23.3	23.3
$-Y$	0.065	7,570	1.35	7,770	10.2	1.99	0.10	0.24	2.26	23.1	23.1

$F_y/(m \cdot g)$ = maximum base shear ratio, m^* = mass of the SDOF system, Γ = transformation factor, F_y^* = ultimate strength of the idealized SDOF system, d_y^* = yield displacement of the SDOF system, T^* = period of the idealized system, S_{ay} (g) = acceleration at the yield point of the SDOF system (F_y^*/m^*), S_{ae} (g) = elastic spectral acceleration at the period T^*, q_u = reduction factor (S_{ae}/S_{ay}), μ = ductility demand, d_{et}^* = target displacement assuming unlimited elastic behaviour, d_t^* = target displacement of the SDOF system

Table 4 The target displacements (d_t) obtained with the N2 method, and comparison with the results of non-linear response-history analyses

Method	Direction X d_t (cm)	Direction Y d_t (cm)
N2	26.0	31.4
Response—history (non-linear)		
Mean	23.4	26.1
Mean + σ	28.7	34.5
Envelope	35.2	48.9

defined with the mean elastic acceleration response spectrum in AD format. The capacity curves and the elastic and inelastic spectra are shown in Fig. 12.

All of the effective periods are, without doubt, larger than the characteristic period of the ground motion (typically $T_C = 0.6$ s for soil type C). The equal displacement rule can therefore be applied to the determination of seismic demand in the case of all of the pushover analyses. Consequently, the inelastic displacement demand is equal to the elastic displacement demand. The displacement demands for the equivalent SDOF system amount to $d_t^* = 0.193$ and 0.233 m in the X and $-Y$ directions, respectively, whereas the corresponding displacement ductility demand (taking into account the yield point of the idealized bilinear system) amounts to $\mu = 2.21$ and 2.26. The corresponding inelastic spectra are plotted, for illustration, in Fig. 12.

In the final step of the basic N2 method, the displacement demands for the equivalent SDOF system were transformed back to the top displacements of the MDOF system. Using the transformation factor $\Gamma = 1.35$, the target displacements amounted to $d_t = 0.260$ m and to $d_t = 0.313$ m for the X and $-Y$ directions, respectively. The target displacement for the $+Y$ direction is practically the same, and amounts to 0.0314 m. A summary of the results obtained by the N2 method is presented in Table 3.

A comparison of the target displacements calculated by the N2 method with the results of non-linear dynamic analyses is presented in Table 4, from which it can be seen that the N2 displacements are within the range between the mean and mean + σ values.

6.3 Torsional effects in terms of the normalized roof displacements.

The torsional effects in terms of the normalized roof displacements u/u_{CM} (i.e. the roof displacement at a location in the horizontal plane divided by the displacement at the CM) determined by the extended N2 method are presented in Fig. 13 The N2 results are compared

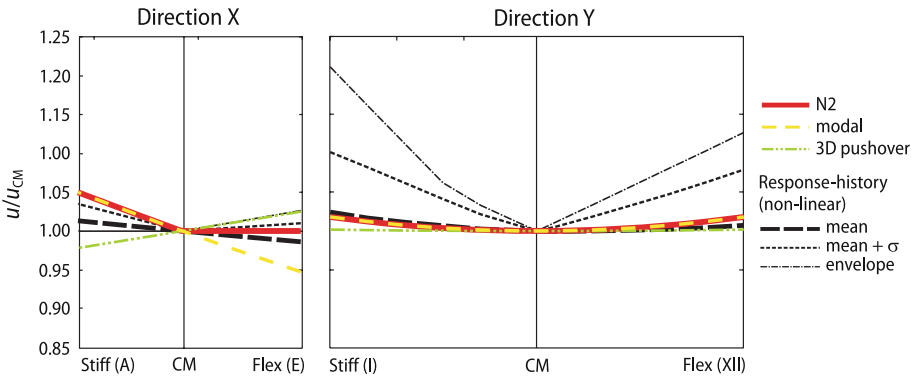

Fig. 13 Torsional effects in terms of the normalized top displacements obtained by different analyses

with the results of non-linear response-history analyses and the usual 3D pushover analyses (SRSS combination of results obtained by two independent analyses in two horizontal directions).

According to the extended N2 method, the results of the elastic modal analysis are used to determine the torsional effect, provided that an amplification due to torsion occurs. No reduction of displacements due to torsion is applied in the N2 method. Consequently, the N2 results coincide with the line obtained by the elastic modal analysis if the normalized displacements are larger than 1.0, whereas the normalized displacements are equal to 1.0 in other parts of the plan (Fig. 13). Modal analysis was performed independently for the ground excitation in each horizontal direction, using the CQC rule for the combination of different modes. The results of the analyses for both directions were combined by the SRSS rule. The mean spectrum (Fig. 7) was used for both directions.

The building is torsionally flexible (see Sect. 6.1). Nevertheless, Fig. 13 indicates that the torsional effects are, on average, small. The maximum torsional amplification, determined according to the extended N2 method (i.e. according to elastic modal analysis), amounts to about 5% at the stiff edge in the X direction, and to about 2% at both edges in Y direction. In the Y direction, good agreement can be observed between the results obtained by using the N2 method and the mean results of the non-linear dynamic analyses, especially on the stiff side. In the X direction, the N2 estimates are within the range between the mean and mean$+\sigma$ values on the flexible side, and close to the envelope on the stiff side. (For definitions of "stiff" and "flexible" sides, see Fig. 4.) The usual pushover analysis of the 3D model yields very small torsional rotations in the Y direction (the building is symmetric with regard to its Y axis, and the very small rotation is due to loading in the X-direction). The pushover results in the X direction coincide with the envelope values corresponding to the flexible side. On the stiff side, a torsional de-amplification is predicted by static pushover analysis instead of an amplification which is predicted by the more accurate dynamic analysis. Torsional amplification on the stiff side typically occurs in torsionally flexible structures.

According to the extended N2 method, the results of pushover analysis are multiplied by correction factors which depend on the location of the elements. The correction factor (c_T) is defined as the ratio between the normalized top displacements obtained by the N2 method and those obtained by pushover analysis. Practically equal correction factors apply to the positive and negative signs of force distributions in the Y direction. The highest values of the correction factors amount to $c_T = 1.07$ and 1.02 for frame A in the X direction, and

for frame I (frame XII) in the Y direction (Fig. 4), respectively. In the X direction, on the flexible side (frame E), the correction factor is smaller than 1.0 ($c_T = 1.0/1.02 = 0.98$). This happens because the torsional amplification by pushover analysis is larger than 1.0, whereas the modal analysis suggests a de-amplification, which is not taken into account in the extended N2 method. The alternative procedure would be to perform a pushover analysis of the building model by assuming planar behaviour of the structure, i.e. with excluded torsional effects (i.e. normalized X displacements equal to 1.0 in all the structural elements) and to determine correction factors based on these results.

In the seismic assessment (Sect. 8) it will be shown that cores are critical structural elements. Due to their position in the plan their torsional amplification is negligible and has not been taken into account in the analyses.

Accidental eccentricity, too, was not taken into account in the analyses presented in this paper. Some earlier studies indicated that accidental eccentricity may substantially increase the torsional effects, especially on the stiff sides (Kreslin et al. 2008).

6.4 Determination of seismic demands

In order to determine the seismic demand, all the relevant quantities corresponding to the target displacements in both horizontal directions, determined by the pushover analyses of the 3D model, were multiplied by appropriate correction factors. A comparison of all of the relevant quantities (i.e. the absolute displacements, the storey drifts, and the demand/capacity ratios at different locations) obtained by extended N2 method and by non-linear dynamic analyses is shown in Figs. 14, 15 and 17. The N2 quantities were calculated as the envelope of the results obtained by pushing from left to right and in the opposite direction.

The absolute values of the roof displacements are plotted in Fig. 14. The N2 displacements in both directions are within the range from the mean to the mean$+\sigma$ values obtained by non-linear dynamic analyses. The torsional amplifications are small.

In Fig. 15 the storey drifts (storey displacement / storey height) are compared. Because of the small torsional amplifications (see Sect. 6.3) the results are presented only for one central location in the plan (on axis C for the X direction, and on axis VII for the Y direction). The N2 estimates are mostly larger than the mean values of the non-linear dynamic analyses, with the exception of the lower stories in the Y direction, where the storey drifts are somewhat underestimated. The drifts increase with the height of the building, indicating

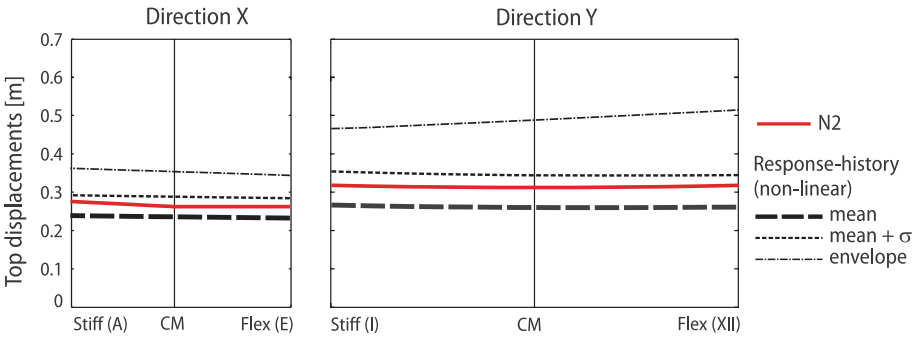

Fig. 14 Displacements (in the *horizontal plane*) at the roof obtained by the extended N2 method and by non-linear dynamic analyses

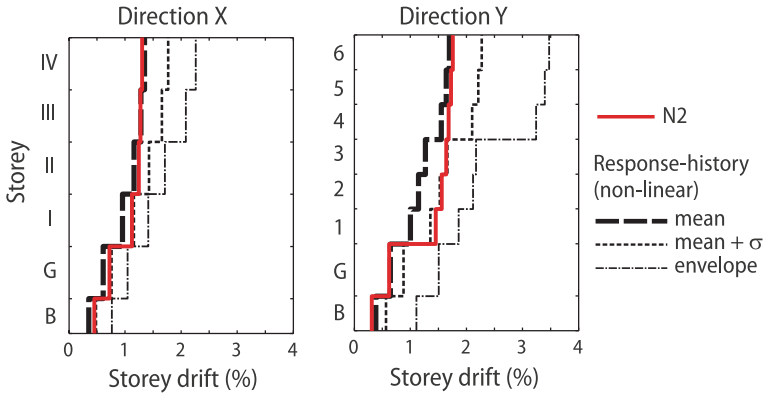

Fig. 15 Storey drifts at axis C for the *X* direction and at axis VII for the *Y* direction, obtained by the extended N2 method and non-linear dynamic analyses

that the overall structural behaviour is dominated by the structural walls. For the walls, the difference between the storey drifts in two neighbouring stories is more important than the absolute value of the storey drift. The largest increase in storey drifts obtained by the N2 method occurs at storey 1. This is the critical part of the structure, which is correctly discovered by the pushover analysis. However, as usual in pushover analyses, the deformations of the critical part of the structure increase disproportionally with increasing roof deformations after yielding of the critical parts, whereas the other potential critical parts of the structure may not be detected. In the case of the investigated structure, non-linear dynamic analyses do not suggest such a large increase in the storey drift at storey 1. However, they indicate substantial increases in storey drifts also at storey 3, where the higher modes seem to be important. Some data on seismic demand in terms of plastic hinge rotations are provided in Sect. 8.

7 Seismic capacity

In different standards and codes, different limit states or performance levels are defined. In this paper, only the near collapse (NC) limit state according to the European standard EC8-3 was considered. Capacities are defined at the element level. There is a lack of the definition of the limit state at the level of the structure. It was assumed in this study that the most critical elements, e.g. the cores (walls), control the state of the structure, i.e. that the NC state of the structure corresponds to the first NC state of a wall.

The flexural capacity of the structural elements was determined according to EC8-3. Equation A.3 in EC8-3 was used. The values for the ultimate plastic chord rotation $\theta_{\mathrm{um}}^{\mathrm{pl}}$, which apply to the secondary elements, were taken into account, because they correspond to the mean values. In the investigated structure, members without detailing for seismic resistance were used. So, the value $\theta_{\mathrm{um}}^{\mathrm{pl}}$ obtained by expression (A.3) was multiplied by a factor of 0.825, which is the value suggested in EC8-3. For the walls, the value of the ultimate plastic rotation $\theta_{\mathrm{um}}^{\mathrm{pl}}$ was multiplied by a factor of 0.6. The ultimate plastic chord rotation for the critical elements, e.g. for the walls at the base (L-0) and at level 2 for both directions, are summarized in Table 5. They amount to between 1.2 and 1.6%. The ultimate plastic chord rotations for the beams are in the range between 3.7 and 6.2%, and for the columns in the

Table 5 Local capacity (upper bound) in terms of the plastic part of the ultimate chord rotation (in %) of the walls according to EC8-3. The locations of the walls and levels are marked in Figs. 4 and 17, respectively

	Level L-0	Level L-2
Small core (direction X)	1.6	1.3
Large core (direction X)	1.5	1.2
Small core (direction Y)	1.5	1.6
Large core (direction Y)	1.6	1.4

Table 6 Shear strengths of the critical elements (small and large cores at the base) obtained according to EC8-3 (secondary elements)

Displacement ductility	Small core (direction X) (kN)	Large core (direction X) (kN)	Small core (direction Y) (kN)	Large core (direction Y) (kN)
1	1,640	2,050	1,350	1,190
4	1,500	1,890	1,230	1,100
6 And more	1,410	1,780	1,150	1,040

range between 1.8 and 6.7%. These estimates are considered as representatives for an upper bound of the flexural capacities. As a lower bound, the values were multiplied by a factor of 0.375 (instead of 0.825), which is used, according to EC8-3, for members with smooth (plain) longitudinal bars without lapping in the vicinity of the end region where yielding is expected.

The shear capacity of the structural elements was also determined according to EC8-3. Equation A.12 was used. In this case, too, the values of the shear strength which apply to the secondary elements were taken into account. The estimated values of the shear strengths at the base for the critical elements, i.e. for the walls in both directions, are summarized in Table 6. For the small core at the base in the Y direction, shear strength is plotted as a function of ductility in Fig. 16.

For comparison, the shear strength of one of the most critical elements (e.g. a small core at the base) was also determined by the other approaches mentioned in Sect. 2.2 (Fig. 16). The

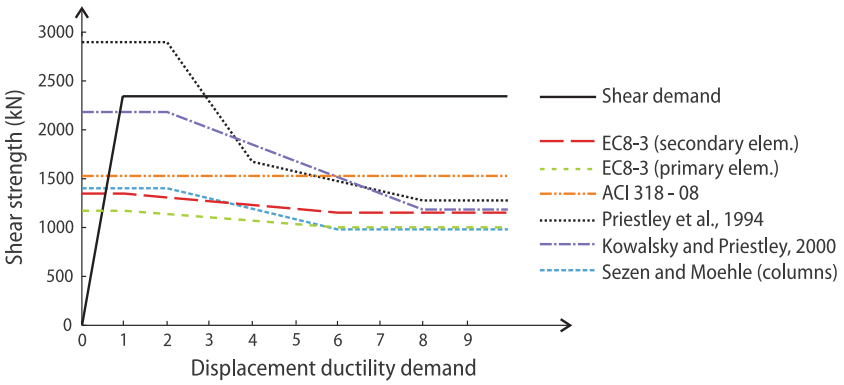

Fig. 16 Comparison of shear demand and shear strength (obtained by different approaches) for the small core at the base in the Y direction

different approaches yield quite different values, especially in the region of small displacement ductility demands. In this region the values obtained according to EC8-3 (secondary elements) are comparable with the values obtained by ACI 318-08 (2007) and with the model for the shear strength of *columns* proposed by Sezen and Moehle (2005). Large differences in the results suggest a large uncertainty in the determination of the shear strength.

8 Comparison of seismic demand and capacity

Figure 17 shows the locations of the plastic hinges and the demand/capacity ratios for frame XII (at the flexible edge) in the *Y* direction and for the cores (walls) in both directions obtained by the N2 method and by non-linear response-history analyses. Upper bound estimates were used for capacities. The N2 analysis was, in general, able to provide a fair estimate of the locations and amplitudes of the plastic rotations. The results indicate that the most critical structural parts are the cores in the *Y* direction at level L-2 (storey 1) where a change in the structural system occurs. (The levels are marked in Figs. 3 and 17). This is consistent with the results in terms of the storey drifts shown in Fig. 15 and is discussed in Sect. 6.4.

The flexural capacity to demand ratio in Fig. 14 indicates that the capacity of all elements is greater than the demand corresponding to the design ground motion. The most critical elements are the two cores in the *Y* direction, where the demand/capacity ratio is the largest. The maximum ratio obtained by the N2 method amounts to $0.009/0.014 = 0.6$. It applies to the large core in the *Y* direction. It is much larger than the mean ratio obtained by non-linear dynamic analyses (0.2), but is still inside the envelope of the non-linear dynamic results (Fig. 17).

The N2 analyses also detected the great majority of plastic hinges throughout the structure, with the exception of the plastic rotations of the cores at storey 4 in the *Y* direction. An advanced pushover method taking into account higher mode effects would be needed to detect this potentially critical part of the structure.

In the further text the discussion will concentrate only on the cores. It will be shown that their shear capacity is not adequate to accommodate the demand.

A comparison between demand and capacity in terms of shear strength shows that the shear in the cores is more critical than flexure. In Fig. 16 the demand in terms of shear force for the small core at the base in the *Y* direction can be compared with the shear strength determined by the different approaches. It can be seen that the demand curve intersects all of the estimated shear capacity curves. Most of the intersections, indicating a shear failure, are already in the elastic region (before the yielding of the longitudinal bars occurs). Only if the shear strength is determined by the procedure proposed by Priestley et al. (1994) can a combined flexural-shear failure be expected.

The global structural response can be visualized by indicating the demand and capacity on the pushover curves. It is important to note that in the non-linear static analyses which were used for the determination of pushover curves it was assumed that the shear capacity of the structural elements is adequate and that shear failures of structural elements do not occur. In the element models, only the flexural behaviour was modelled. The increased ultimate flexural capacity of the RC elements in terms of the plastic part of the chord rotations was considered in the mathematical models for the plastic hinges (see Sect. 4). In such a way, pushover curves were obtained which extend into the range of large deformations. Different alternatives for capacities can be easily investigated. Of course, the pushover curve is actually valid only up to the deformation or strength corresponding to the NC capacity of the

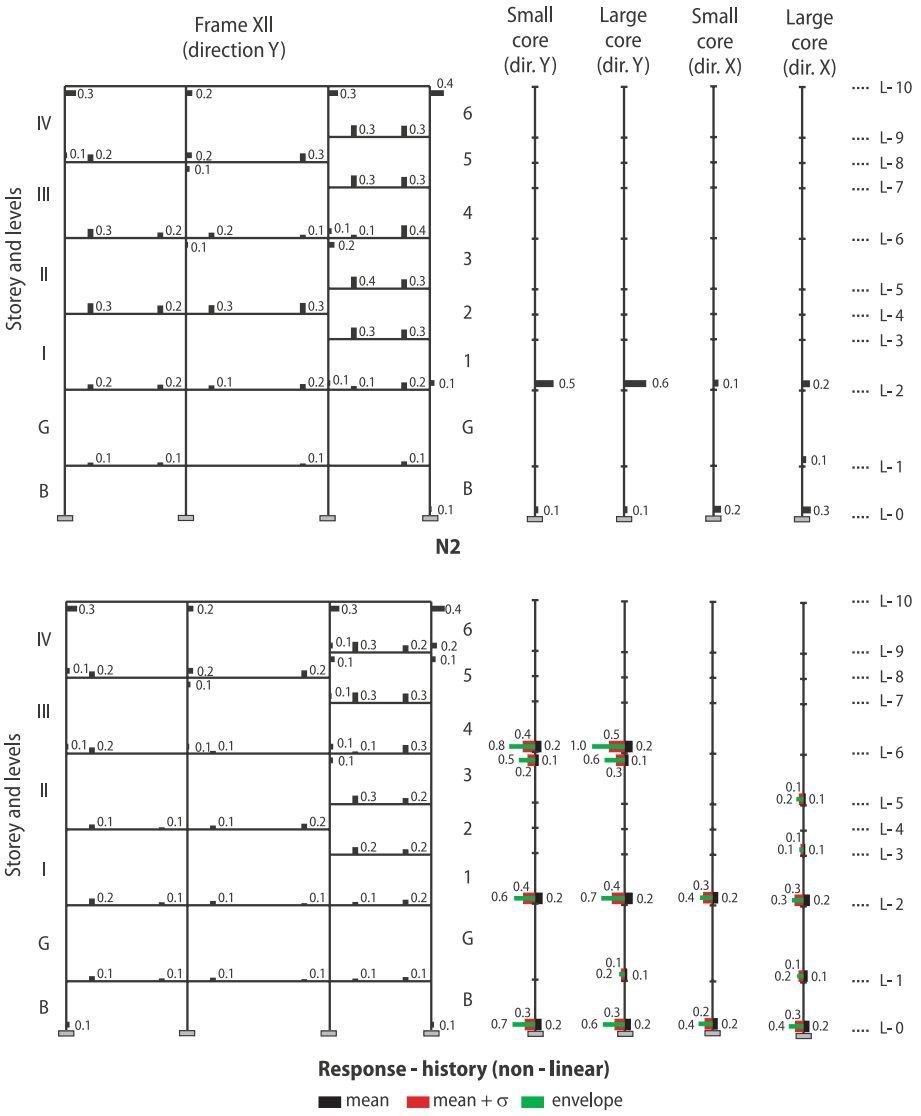

Fig. 17 The locations of the plastic hinges and the demand/capacity ratios for selected elements (frame XII in the *Y* direction and the cores in both directions). The demands were obtained by the extended N2 method and by non-linear dynamic analyses (mean, mean + σ, envelope). The flexural capacities of the elements were calculated according to EC8-3 (*upper bound*)

first structural element. After this point the structural element starts to degrade or even fails, which means the whole structural model would need to be changed.

In the presented example, the NC limit states for flexural and shear failure were treated separately. Interaction between bending moment and shear force was not taken into account. It was assumed that the NC limit state of the structure occurs when the NC limit state of the critical element is reached. Both the plastic part of the chord rotation (the NC limit state for flexure) and the shear strength (the NC limit state for shear) were checked.

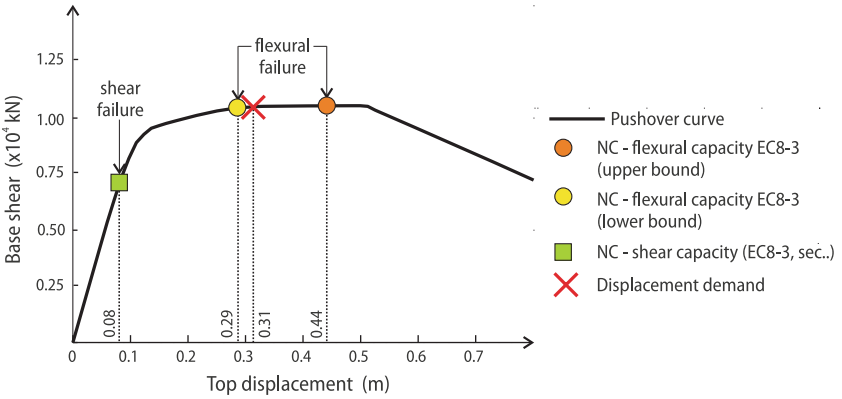

Fig. 18 Pushover curve for the negative Y direction. The displacement demand and the NC limit states (flexural and shear failure) are indicated

The results are presented using a pushover curve for the whole structure (top displacement at the mass centre versus base shear). For a structure with negligible torsion, as in the investigated case, the top displacement in the pushover curve applies to the top displacements of all of the structural elements. If torsion is taken into account, there is a fixed factor between top displacements at the mass centre and at the location of specific elements. This factor has to be taken into account when presenting the results.

Figure 18 indicates the displacement demands and NC capacities based on the NC limit state of the small core for the negative Y direction, which is the most critical element for flexural failure. The shear failure is critical for both cores in the X and Y directions. The displacements at the top of the small core (which, due to negligible torsion, are practically equal to the top displacement at the mass centre) for the NC limit state amount to 8.2 cm (shear failure), to 28.6 cm (flexural failure—lower bound), and to 44.2 cm (flexural failure—upper bound). The displacement demand (displacement at the top of the selected element) corresponding to the effective design seismic action ($a_g = 0.345$ g) for type C soil amounts to 31.3 cm. A comparison of the capacities and demands has shown that shear is much more critical than flexure. If the shear capacity is calculated according to EC8-3, shear failure occurs already in the elastic region. The most critical is the section at the base. If the shear strength was calculated according to other approaches instead of EC8-3, the shear failure would occur at a later stage, but still in the elastic region, with one exception (see Fig. 16). Assuming that shear failures are prevented (e.g. by strengthening measures) and that flexure governs the structural behaviour, the most critical section of the small core is in the Y direction at level 2, where a change of the structural system occurs. In such a case, the structure would most probably survive the design earthquake according to EC8.

Using the steps of the N2 method in a different order (starting from the target displacement corresponding the roof displacement at flexural failure) it is possible to determine the spectral acceleration S_{ae} corresponding to the roof displacement at flexural failure. For a known shape of the acceleration spectrum it is then possible to determine the corresponding effective design acceleration a_g which the structure is able to survive. In the case of the EC8 spectrum for type C soil, it amounts to $a_g = 0.09$ g ($S_{ae} = 0.09$ g). If the shear capacity was adequate, the maximum effective design acceleration would amount to $a_g = 0.31$ g ($S_{ae} = 0.30$ g) and

to $a_g = 0.49$ g ($S_{ae} = 0.47$ g) for the minimum and maximum value of the flexural capacity, respectively.

9 Conclusions

A procedure based on the N2 method (which has been implemented in Eurocode 8) was used for the seismic evaluation of an existing irregular RC building. The procedure generally follows the Eurocode 8 approach, but is not completely in compliance with it. In order to obtain a realistic estimate of the seismic resistance of the building, best estimates for the material parameters and capacities were intentionally used, rather than the low fractile values required by Eurocode 8 and other codes. The procedure proved to be a feasible tool for the seismic evaluation of a complex multi-storey building structure. Comparisons between the results obtained by the N2 method and those obtained by non-linear dynamic analyses suggest that the N2 method provides a reasonable estimate for the seismic demands (considering the large inherited dispersion) which is conservative in the majority of cases. Data on seismic capacity are mostly empirical or semi-empirical, and are available in different standards, codes and other literature. Quite large differences between data from different sources exist. A comparison of the demands and capacities suggests, as expected, that the structure would fail when subjected to the design seismic action according to Eurocode 8. As expected for an existing RC concrete building with an insufficient amount of transverse steel, the most critical parameter is the shear capacity of the structural walls. However, if the shear capacity of the structural elements were to be adequate, the structure would, due to its large overstrength, be able to survive the design ground motion according to Eurocode 8 in spite of the very low level of the design horizontal forces.

The application to real complex structures of different evaluation procedures, which have been usually tested on highly idealized structural models is by no means straightforward. Also the application of standards and codes (e.g. Eurocode 8, Part 3) is a demanding task which can be adequately performed only by a well educated and experienced designer. In the literature, different procedures for seismic evaluation are usually applied to highly idealized structures. In practice, if a seismic evaluation approach is applied to a complex structure, several problems may occur which require professional decisions and reasonable solutions. The problems encountered in the case of the investigated structure include, inter alia, the choice of a rational mathematical model, which is also related to the choice of the computer program, the modelling of effective widths and of cracked element sections, the treatment of accidental eccentricity, determination of capacities at member level, and definitions of limit states at the level of the complete structure. In some cases, guidance is provided in codes. However, the requirements in different codes are often quite different (see e.g. the comparative study by Lupoi et al. 2004), and in all cases a considerable degree of conservatism is involved.

The seismic evaluation of existing buildings is a more difficult task than the seismic design of new buildings. Non-linear methods are needed in order to obtain realistic results. However, even if the most advanced and sophisticated methods are used, structural response to strong earthquake ground motion cannot be accurately predicted due to the large uncertainties and randomness of the structural properties and the ground motion parameters. Consequently, excessive sophistication in structural analysis is not warranted. The N2 method, like some other simplified non-linear methods, provides, in combination with data on seismic capacity, a feasible tool for the rational yet practical seismic evaluation of building structures for multiple performance objectives. Formulation of the method in the acceleration—-displace-

ment format enables visual interpretation of the procedure and of the relations between the basic quantities controlling the seismic response. This feature is attractive to designers.

Acknowledgments The work presented in this paper was supported by the Slovenian Research Agency.

References

ACI 318-08 (2007) Building code requirements for structural concrete and commentar. An ACI standard, American Concrete Institute, Farmington Hills

Ambraseys N, Smit P, Sigbjörnsson R, Suhadolc P, Margaris B (2002) Internet-site for European strong-motion data. European Commission, Directorate-General XII, Environmental and Climate Programme, Brussels. http://www.isesd.cv.ic.ac.uk

Bardakis VG, Dritsos SE (2007) Evaluating assumptions for seismic assessment of existing buildnig. Soil Dyn Earthq Eng 27:223–233. doi:10.1016/j.soildyn.2006.07.001

Calvi GM, Pavese A, Rasulo A, Bolognini D (2005) Experimental and numerical studies on the seismic response of R.C. hollow bridge piers. Bull Earthq Eng 3:67–297. doi:10.1007/s10518-005-2240-0

CEN (2004) Eurocode 8—design of structures for earthquake resistance. Part 1: general rules, seismic actions and rules for buildings. European standard EN 1998-1, December 2004, European Committee for Standardization, Brussels

CEN (2005) Eurocode 8—design of structures for earthquake resistance. Part 3: assessment and retrofitting of buildings. European standard EN 1998-3. June 2005. European Committee for Standardization, Brussels

CSI (2006) PERFORM 3D nonlinear analysis and performance assessment for 3D structures. Computers & Structures Inc, Berkeley

FEMA 356 (2000) Prestandard and commentary for the seismic rehabilitation of buildings. Federal Emergency Management Agency, Washington

Fajfar P (2000) A nonlinear analysis method for performance-based seismic design. Earthq Spectra 16(3):573–592. doi:10.1193/1.1586128

Fajfar P, Marušić D, Peruš I (2005) Torsional effects in the pushover-based seismic analysis of buildings. J Earthq Eng 9(6):831–854. doi:10.1080/13632460509350568

Ghobarah A (2000) Seismic assessment of existing structures. Prog Struct Eng Mater 2(1):60–71

Isaković T, Bevc L, Fischinger M (2008) Modeling the cyclic flexural and shear response of the R. C. hollow box columns of an existing viaduct. J Earthq Eng 12(7):1120–1138. doi:10.1080/13632460802003587

Kowalsky MJ, Priestley MJN (2000) Improved analytical model for shear strength of circular reinforced concrete columns in seismic regions. ACI Struct J 97:388–396

Kreslin M, Dolšek M, Fajfar P (2006) Matematično modeliranje in analiza armiranobetonske stavbe po EC8 = mathematical modeling and analysis of a reinforced concrete building according to EC8. Gradbeni vestnik (in Slovenian) 55(6):141–152

Kreslin M, Dolšek M, Fajfar P (2008) Seismic analyses of an irregular existing RC building. In: Proceedings of the Workshop on the seismic behaviour of Irregular and Complex Structures. Catania

Lupoi G, Calvi GM, Lupoi A, Pinto PE (2004) Comparison of different aproaches for seismic assessment of existing buildings. J Earthq Eng 8(1):121–160. doi:10.1142/S1363246904001626

Mergos PE, Kappos AJ (2008) A distributed shear and flexural flexibility model with shear—flexure interaction for R/C members subjected to seismic loading. Earthq Eng Struct Dyn 37(12): 1349–1370. doi:10.1002/eqe.812

Panagiotakos TB, Fardis MN (2004) Seismic performance of RC frame designed to Eurocode 8 or to the Greek Codes 2000. Bull Earthq Eng 2:221–259. doi:10.1007/s10518-004-2288-2

Peruš I, Poljanšek K, Fajfar P (2006) Flexural deformation capacity of rectangular RC columns in flexure by the CAE method. Earthq Eng Struct Dyn 35(12):1453–1470. doi:10.1002/eqe.584

Priestley MJN, Verma R, Xiao Y (1994) Seismic shear strength of reinforced concrete columns. J Struct Eng ASCE 120(8):2310–2329. doi:10.1061/(ASCE)0733-9445(1994)120:8(2310)

Sezen H, Moehle JP (2005) Shear strength model for lightly reinforced concrete columns. ACI Struct J 130(11):1692–1703. doi:10.1061/(ASCE)0733-9445(2004)130:11(1692)